Characterisation of the ALICE Accelerator as an Injector for the EMMA NS-FFAG*

J.M. Garland†, H.L. Owen, Manchester University and Cockcroft Institute
B.D. Muratori, J.W. McKenzie, STFC Daresbury Laboratory, ASTeC and Cockcroft Institute

Abstract

EMMA (Electron Model with Many Applications) is the first proof-of-principle non-scaling FFAG accelerator and is presently under construction at Daresbury Laboratory in the UK. To probe different parts of the bunch phase space during the acceleration from 10 to 20 MeV (which requires rapid resonance crossing), electron bunches are needed with sufficiently small emittance. To understand the phase space painting into the 3000 mm-mrad EMMA acceptance, we have modelled ALICE (Accelerators and Lasers in Combined Experiments) - which acts as an injector for EMMA - using GPT and compared the estimated emittances with measurements made with a variety of screen-based methods. Although the emittances are not yet as small as desired, we obtain reasonable agreement between simulation and measurement.

INTRODUCTION

Figure 1 shows the layout of the ALICE injector, which is to be used as an electron source for EMMA [1, 2, 3]; electron bunches must be provided with transverse and longitudinal sizes much smaller than the EMMA acceptance to allow effective phase space exploration [3, 4, 5]. Electron bunches are accelerated to 6.5 MeV in the 'Booster' accelerating module, composed of two 1.3 GHz TESLA-type superconducting cavities [6, 7, 8]. The transverse emittance should not grow significantly after the ALICE injector; the emittance measured directly after the injector should be approximately that delivered to EMMA.

GPT SIMULATIONS

We have modelled the ALICE injector line using GPT [12] with a fast 3D space-charge mesh calculation. The present injector laser setup results in an more-or-less elliptical cathode distribution approximately 8 mm in y and 4 mm in x (Figure 2). We have simulated both a hard-edged distribution and a distribution based on the measured cathode spot (see Figure 3). In both cases, we generate a transverse distribution using rejection sampling to populate the distribution according to the desired probability density function (PDF); the longitudinal coordinate (release time) is modelled as a uniform distribution (which the real pulse is close to being [9]) with pseudo-random sampling. Results are shown in Table 2.

The predicted emittance is rather sensitive to the overall spot size scale, and hence is sensitive to any calibration error in the spot size measurement: an accurate spot size calibration is difficult to determine due with the presently available diagnostics. However, the eccentricity in the initial distribution is well predicted by the model. Figure 4

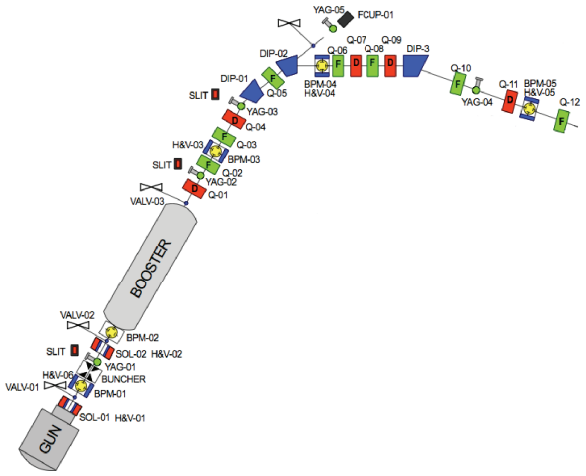

Figure 1: Layout of the ALICE injector. A 350 kV DC GaAs photocathode is followed by a 2-solenoid emittance matching section, buncher, and 2-cavity TESLA-type accelerating module [8].

Table 1: Beam parameters at the cathode [9].

Charge	40 pC
Pulse Length	28 ps
Ideal Circular Spot Diameter	4 mm
Present Elliptical Spot	8x4 mm
Final Energy	6.5 MeV

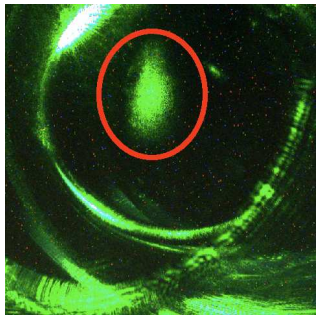

Figure 2: Captured image showing measured laser spot at the ALICE cathode (other reflections are visible). The cathode spot is circled in red.

* Work supported by an STFC CASE award
† james.garland@hep.manchester.ac.uk

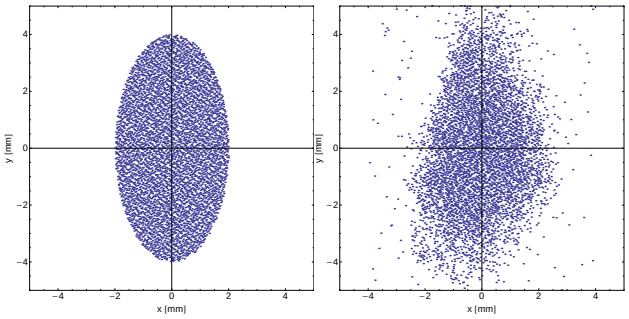

Figure 3: Elliptical and 'real spot' distributions generated for GPT. Macroparticles are distributed transversely using a 2D Halton sequence according to the PDF for each distribution, using von Neumann rejection sampling. 5000 particles are shown here; 10000 are used in the simulations

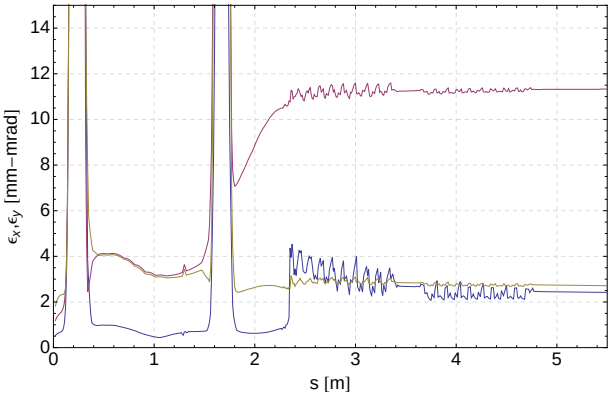

Figure 4: Evolution of beam emittance for round (blue) and an upright elliptical (red/green) cathode laser spots with equal area $\pi \times 2\text{mm}^2$, the elliptical beam having 2:1 vertical/horizontal spot dimensions. The upright elliptical distribution results in a vertical emittance similar to that from a round spot, but gives a much-increased horizontal emittance.

compares the evolution of cathode spots of equal area but different eccentricities (one round, one elliptical), showing the rotation from upright to flat. Figure 5 shows the variation of predicted emittance with spot shape.

TRANSVERSE EMITTANCE MEASUREMENTS

Several measurement techniques were used to determine the transverse emittance in the ALICE injector using the same 40 pC operating conditions as for the simulation above.

Single Slit Position

Beam images were recorded on two YAG screens a distance d apart with all intervening magnets turned off in. A 10μm tungsten slit is inserted in place of the upstream YAG screen when measuring the downstream YAG image. The

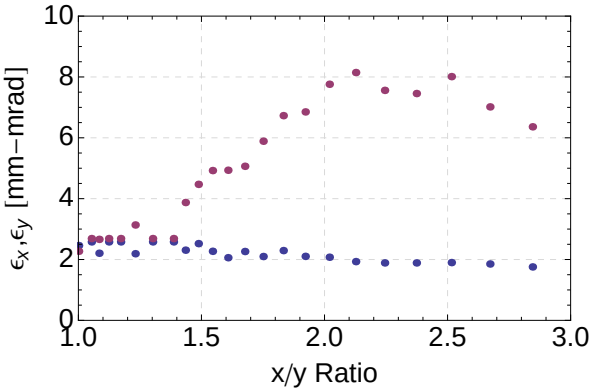

Figure 5: Variation of final emittance with initial cathode spot size ratio, for a hard-edged elliptical distribution. An ratio of $\sigma_y/\sigma_x = 2$ at the cathode gives a $\sigma_x/\sigma_y = 3$ (i.e. rotated) at the injector end.

RMS beam size, σ was determined by fitting a Gaussian to the mean of the transverse intensity profile in x. Figure 6 gives example images on the two YAG screens with their corresponding Gaussian intensity profiles. The normalised emittance ϵ_n in the x plane is calculated as

$$\epsilon_n = \frac{\sigma_{YAG2} \cdot \sigma_{YAG3}}{d} \cdot \gamma, \qquad (1)$$

where the distance between the YAG screens is d, σ is the RMS horizontal beam size on each screen. The horizontal emittance was determined to be 11.0 mm.mrad.

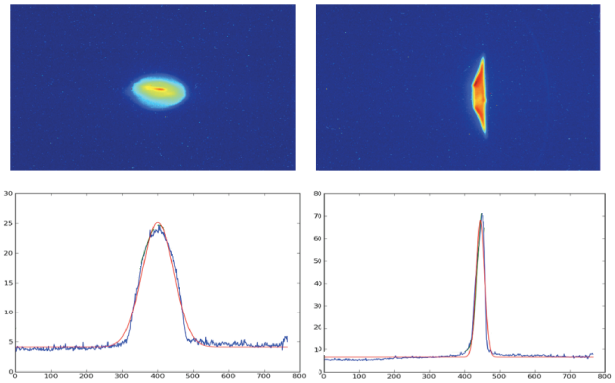

Figure 6: Examples of YAG images of the beam with corresponding intensity profiles and Gaussian fits. The left shows the upstream YAG image, the right the downstream YAG after the vertical slit has been inserted in place of the upstream screen.

Slit Scan

This technique is similar to the single slit position measurement, but instead the slit is scanned across the beam and many beamlet images are recorded at the downstream

YAG screen. From the intensity profile of the beamlet images we can reconstruct the position and the uncorrelated divergence of the beam at the witness YAG screen and calculate the normalised emittance using the standard formula:

$$\epsilon_n = \sqrt{< x^2 >< x'^2 > - < xx' >^2} \cdot \gamma, \qquad (2)$$

where $< x^2 >$ is the square of the RMS beam size, $< x'^2 >$ is the square of the beam divergence and $< xx' >^2$ is the cross correlation term. Using this method the normalised transverse emittance in the x plane was determined to be 9.1 mm.mrad.

Quadrupole Scan

Two suitable quadrupoles (one F, one D) immediately downstream of the booster module were each scanned separately to determine the transverse emittances; a typical measurement is shown in Figure 7. The resulting beam sizes were fitted using the parameterisation

$$< x^2 >= A(kL)^2 - 2AB(kL) + (C + AB^2) \qquad (3)$$

where $< x^2 >$ is the square of the RMS beam size, kL the integrated quadrupole field, and A, B and C are polynomial fitting constants. The emittance is then determined as

$$\epsilon_n = \frac{\sqrt{A \cdot C}}{d^2} \cdot \gamma \qquad (4)$$

where d is the distance between the quadrupole magnet used and the YAG screen. The normalised transverse emittances were found to be 15.1 mm.mrad in x and 4.0 mm.mrad in y.

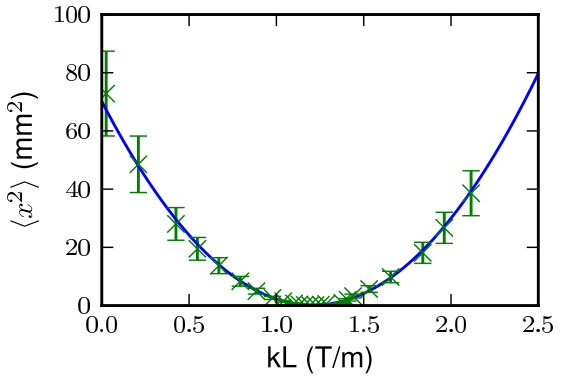

Figure 7: An example of $< x^2 >$ vs. kL for a quadrupole scan, showing the resulting polynomial fit in blue. The error on the beam size is rather large: approximately 20%.

SUMMARY

The measurement and simulation results are summarised in Table 2. There is reasonable agreement between the quadrupole scan measurements and GPT simulations using a reconstructed transverse spot, but uncertainties in the transverse size calibration and longitudinal distribution remain. We intend to improve our understanding of the slit-based measurements to resolve the present discrepancy. However, we have shown that the present overly-large horizontal emittance is explained by the elliptical cathode distribution, and that the injector performance can be made better by improving the cathode spot symmetry.

Table 2: Summary of emiittance measurements and simulations. All values given in mm-mrad.

Result	ϵ_x	ϵ_y
Single Slit	11.0	N/A
Slit Scan	9.1	N/A
Quad Scan	15.1	4.0
Measurement Average	11.7	4.0
GPT (Elliptical)	9.5	1.9
GPT (Real Spot)	17.7	3.8

REFERENCES

[1] R. Edgecock et al., 'EMMA - The Worlds First Non-Scaling FFAG', EPAC08, Genoa (2008).

[2] R.J. Barlow et al., 'The CONFORM Project: Construction of a Nonscaling FFAG and its Applications', PAC'07, Albuquerque (2007).

[3] J.S. Berg et al., 'The EMMA Lattice Design', PAC'07, Albuquerque (2007).

[4] B.D. Muratori et al., 'Injection and Extraction for the EMMA NS-FFAG', EPAC08, Genoa (2008).

[5] T. Yokoi and S. Machida, 'Beam Injection Into EMMA Non-Scaling FFAG', EPAC08, Genoa (2008).

[6] C. Gerth et al., 'Start-to-End Simulations of the Energy Recovery Linac Prototype FEL', FEL'04 (2004).

[7] B.D. Muratori et al., 'Space Charge Effects for the ERL Prototype Injector Line at Daresbury Laboratory', PAC'05, Knoxville (2005).

[8] D. J. Holder et al, 'The Status of ALICE, the Daresbury energy recovery linac prototype', EPAC08, Genoa (2008).

[9] Y. M. Saveliev et al., 'Characterisation of electron bunches from ALICE (ERLP) DC photoinjector gun at two different laser pulse lengths', EPAC08, Genoa (2008).

[10] B.D. Muratori and Y.M. Saveliev, 'ALICE (ERLP) Injector Design', EPAC08, Genoa (2008).

[11] C. Beard et al., 'The Current Status of the ALICE Facility', FEL'09, Liverpool (2009).

[12] S.B. van der Geer and M.J. de Loos, 'General Particle Tracer: a 3D Code for Accelerator and Beam Line Design', EPAC'98, Stockholm (1998). www.jacow.org, www.pulsar.nl/gpt